

INFLUENCE OF ELECTROLYTE THICKNESS ON THE SOLID OXIDE FUEL CELL PERFORMANCE¹

Taisa Eva Fuziger Gutierrez²
José Geraldo de Melo Furtado³

Abstract

Solid oxide fuel cells (SOFC) must have significantly reduced their cost in order to reach entry markets for new technologies for generating electrical power. Thus, there is a technological tendency to reduce the operating temperature of this type of fuel cell of the current 1000-900^oC to 800-650^oC, as this makes assembly and engineering of the device simpler and softens the requirements criteria that the various materials and components must meet. However, as the ionic conductivity of the electrolyte is very dependent on temperature, the thickness of the electrolyte is replaced by a fundamental role as it will determine the power losses of the SOFC generator. In this work, based on microstructural, electrical and electrochemical characterizations, it was investigated the influence of the thickness of the solid electrolyte on the performance of SOFC single cell units and combined anode-electrolyte ceramics. The early results obtained show that it was possible to achieve significant reduction in electrical resistances when the thickness of the electrolyte is also significantly reduced. Good results on the electrical behavior under open circuit voltage and to the 1 A/cm² electrical current density conditions were also obtained.

Key words: Fuel cells; SOFC; solid electrolyte; electrical characterization.

INFLUÊNCIA DA ESPESSURA DO ELETRÓLITO SOBRE O DESEMPENHO DE CÉLULAS A COMBUSTÍVEL DE ÓXIDO SÓLIDO

Resumo

Células a combustível de óxido sólido (SOFC) têm apresentado redução de custos e, por consequência, têm se tornado uma nova opção tecnológica para a geração de energia elétrica. Existe uma tendência tecnológica de redução da temperatura de operação deste tipo de célula a combustível da atual faixa de 1000-900^oC para 800-650^oC, possibilitando uma construção mais simples do dispositivo e reduzindo as exigências que devem ser atendidas pelos seus materiais e componentes constitutivos. Contudo, como a condutividade iônica do eletrólito depende da temperatura, a espessura deste componente passa a desempenhar um papel decisivo nas perdas de potências das SOFC. Neste trabalho, com base na caracterização microestrutural, eletroquímica e elétrica, foi investigado a influência da espessura do eletrólito sólido sobre o desempenho de células unitárias do tipo SOFC e seus conjugados eletrólito-eletrodos. Os resultados obtidos mostram que foi possível alcançar significativa redução da resistência elétrica quando a espessura do eletrólito foi reduzida. Bons resultados acerca do comportamento elétrico em potencial de circuito aberto e em densidade de corrente elétrica igual a 1 A/cm² foram também obtidos.

Palavras-chave: Células a combustível; SOFC; Eletrólito sólido; Caracterização elétrica.

¹ Technical Contribution to the 67th International Congress of the ABM, July 31st to August 3rd, 2012, Rio de Janeiro – RJ – Brazil.

² M.Sc., Fellow Researcher, Special Technologies Department (DTE), Electric Power Research Center, P.O.Box 68007, 21940-970, Rio de Janeiro, Brazil. e-mail: taisa_fuziger@yahoo.com.br

³ D.Sc., Researcher, Special Technologies Department (DTE), Electric Power Research Center, Cepel, P.O.Box 68007, 21940-970, Rio de Janeiro, Brazil. e-mail: furtado@cepel.br

1 INTRODUCTION

Fuel cells are electrochemical devices that, via electrochemical reactions, are able to combine a fuel and an oxidant, converting the stored chemical energy of the fuel directly into direct-current electrical energy and heat as a byproduct. The fuel is not burned (there is no combustion), such as in a flame, as in conventional power generation systems; rather, it is electrochemically oxidized. Thus, the maximum efficiency of a fuel cell is not limited by the Carnot cycle, which limits many conventional power systems such as the internal combustion engines, steam and gas turbines, and heat pumps.⁽¹⁾ Thus, fuel cells have been regarded as the main power generation equipment capable of increasing the energy conversion efficiency and reduce or eliminate the emission of pollutants in various fields of applications.^(2,3)

Solid oxide fuel cell (SOFC), one of the types of fuel cells, is one of the most promising technologies for the production of energy, with potential to be a typical future distributed cogeneration system^(4,5) due to its high energy efficiency, low pollutant emissions, potential fuel flexibility, high modularity as a solid-state device and co-generation capability.^(5,6) Typically, a SOFC system is constituted of at least seven distinct components:⁽⁶⁻⁸⁾ fuel feed, anode, electrolyte media (separating the two electrodes), cathode, oxidant agent feed (normally air), sealing materials and electrical interconnectors (completing the electrical circuit stack) as schematically showed in the Figure 1.

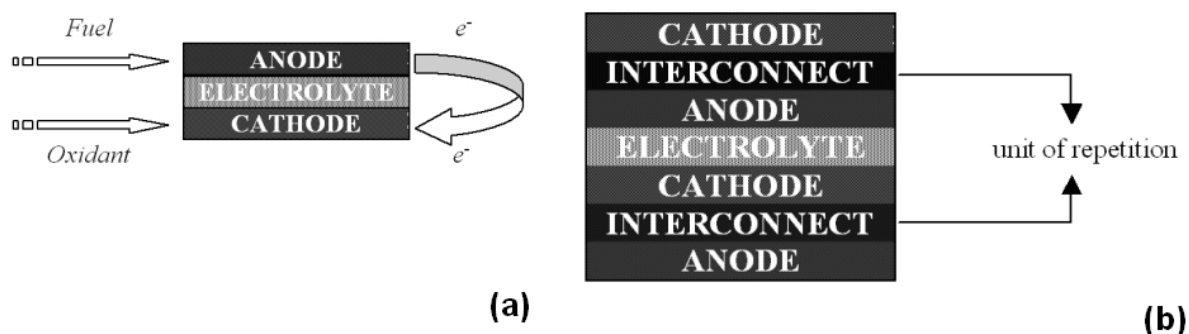


Figure 1. (a) Schematic diagram of a fuel cell; (b) scheme of the connection of the anode of a single fuel cell to the cathode of the subsequent single fuel cell, constituting a solid oxide fuel cell stack.

In SOFC technology, the heart of the fuel cell is a solid-state composite material-device of which emerges the respective electrical fuel cell behavior. This composite component is the Electrolyte-Electrodes Assembly (EEA), also known as MEA (Membrane Electrode Assembly), which is composed by a ceramic electrolyte sandwiched by two electrocatalysts-porous-electrodes, becoming the main component that holding the most significant influence on overall cost, useful life and fuel cell performance.⁽⁸⁻¹⁰⁾ Technologically there is a greater tendency to develop the planar configuration for SOFC systems, and this type of configuration is capable of achieving very high power density^(8,11) characterized by a very thin electrolyte deposited on an anode considerably thicker, but that presents a reaction zone typically five to six times thicker than the ceramic electrolyte.^(6,11) Thus, the electrolyte contribution to the ohmic loss is minimized and the microstructural characteristics of the interfacial electrolyte/anode region become highly relevant to determining the electrical behavior of SOFC, since the electrolyte is responsible for the ohmic

overpotential, resulting in loss of power and efficiency of the SOFC by electrothermal effects.^(1,6, 8,10)

Ceramic electrolytes for SOFC can be synthesized, produced and shaped or conformed by various methods^(6,7) and yttria-stabilized zirconia (YSZ) ceramics, with intermediate ionic conductivity at high temperatures, low electronic conductivity and high chemical stability under oxidizing and reducing atmosphere, are the more common electrolyte used in SOFC.^(6,10,12) Alternative electrolytes have also been much studied, especially in the context of applications of intermediate temperature SOFC (IT-SOFC), and among them, the ceria-based ceramics have shown the best prospects⁽¹³⁻¹⁵⁾. In all cases, whatever the material, besides of the physical and chemical homogeneity, the dimensional characteristics of the electrolyte are important to the performance of the cells and they affect the power loss of a stack. Accordingly, this work aims to study and evaluate the influence of the thickness of ceramic solid electrolytes on the performance of SOFC single cell units and combined anode-electrolyte ceramics, with focus on the analysis performed by microscopy techniques and electrical and electrochemical characterization.

2 EXPERIMENTAL

In this work studies were performed with the ceramic electrolyte materials YSZ and rare-earth-doped ceria (ERC), as well as with systems electrolyte/anode 8YSZ/Ni-YSZ and ERC/NiO, where 8YSZ is yttria-(8mol%)-stabilized zirconia, which are the electrolytes that have been considered for SOFC applications of high (HT-SOFC) and intermediate (IT-SOFC) temperature. The respective ceramic electrolyte powders were synthesized and applied on the anode substrates. Then, the cathode material (lanthanum strontium manganite, LSM) was applied on the electrolytes by a screen printing route.

For the synthesis of 8mol%Y₂O₃-stabilized zirconia (8YSZ) powder, by Pechini's method, the zirconium oxychloride octahydrate (ZrOCl₂.8H₂O) and the yttrium nitrate pentahydrate (Y(NO₃)₃.5H₂O) were dissolved in ethylene glycol, anhydrous citric acid was added in a molar ratio of 1:5 between ethylene glycol and citric acid. The mixture was stirred for about 30 minutes under heating to 80°C, to promote polyesterification. The resulting gel was kept in oven at 180°C for 12 hours. The resulting fine powders were calcined at 900°C for 6h using heating rates of 10°C/min, with air flow rate of 60 mL/min. The ERC system was obtained from acid digestion of praseodymium, dysprosium and yttrium oxides under stirring at 70°C for 48 hours and subsequent them infiltration into the matrix of ceria powder, heated to 120°C and stirring for 24 hours. Suspensions of the respective powders were prepared and deposited by tape casting (8YSZ) and by infiltration method (ERC) on the respective anode materials, producing thus EEA with different thickness electrolyte layers. The complete systems were heat-treated and prepared for characterization.

The microstructures of the samples were examined by scanning electron microscopy (SEM, Jeol JSM-64602 LV) equipped with X-ray dispersive energy spectroscopy (EDS, Link ISIS, Oxford Instruments) for chemical compositional analysis. The electrothermal behavior was measured using a curve tracer source-measurement unit (Tektronix 577) and an Agilent 4294A precision impedance analyzer. The electrochemical performances of the single cells were measured using hydrogen and oxygen analytical grades (99.99% pure), under low pressure (40-50 mbar) conditions, and the ceramic single cells were placed in a metallic cell for

electrothermal testing. In the results presented below, dispersion bars were used when its respective scale so allowed.

3 RESULTS AND DISCUSSION

Figures 2(a) and 2(b) show photomicrographs of the 8YSZ/Ni-YSZ combined anode electrode-electrolyte ceramic and an EDS spectrum (Fig. 2(c)). Both in the Figure 2(a) as in Figure 2(b) it were clearly identifies the regions of the electrolyte and of the anode as a function of their characteristic aspects of the consolidated materials are very different, since the anode is essentially porous, while the electrolyte is essentially dense. In fact, according to the photomicrograph shown in Figure 2(b) it was observed the porous structure of anode and electrolyte microstructures showing clear grain boundaries as a result of high densification, although intra- and mainly intergranular pores are observed, which can be reduced or eliminated by optimizing the sintering.

In Figure 2(a), secondary electrons image, it was note the dimensions involved and, in this case, the thickness of electrolyte is about twenty times lower than that of the respective anode, in this case about 1.3 μm . The microstructural characteristics of the interface electrolyte/anode can also be examined from the photomicrograph of Figure 2(b), backscattered electrons image, in which it appears that although there is some heterogeneity, there was no interpenetration between the layers. Figure 2(c) shows the EDS spectrum characteristic of ceramic combined system shown in Figure 2(a), showing, as expected, only the presence of Zr, Y and Ni.

The results of a detailed profiles EDS microanalysis can be seen in Figure 3, where the composition is chemically analyzed along the yellow line shown on the photomicrography and beginning at a point located within the grain of 8YSZ and ends in the anodic region already distant of the 8YSZ/electrode interface, but yet the typical reaction zone (porous anode structure).

The EDS spectra along said line, for the elements Zr, Y and Ni are shown respectively in Figures 3(b), 3(c) and 3(d) and the results indicate the absence of interpenetration, since Ni essentially it was not detected in the area of the electrolyte (Figure 3d), which presents a partially complementary to the profile of Zr (Figure 3b). After the interface electrolyte/electrode count on Ni is considerably high and, based on the image obtained with backscattered electrons (Figure 3(a)) it was noted that the Ni is well dispersed in the reaction zone. On the other hand, the Y has a profile of amphoteric character, since it is found at comparable levels (slightly higher in the area of the electrolyte) on both sides of the interface electrolyte/anode. The absence of interpenetration of Ni is an indication of suitable conditions of processing, but still need some optimization in order to reduce the porosity remaining in the electrolyte and improve the morphological, structural and compositional characteristics of the interface electrode/electrolyte, because on the one hand, as noted by Nakajo et al.⁽¹⁶⁾ the diffusion of Ni into the electrolyte can lead to failures of SOFC at high temperatures and, on the other hand, porosity is a factor that results in loss of efficiency of the electrolyte.^(6,10)

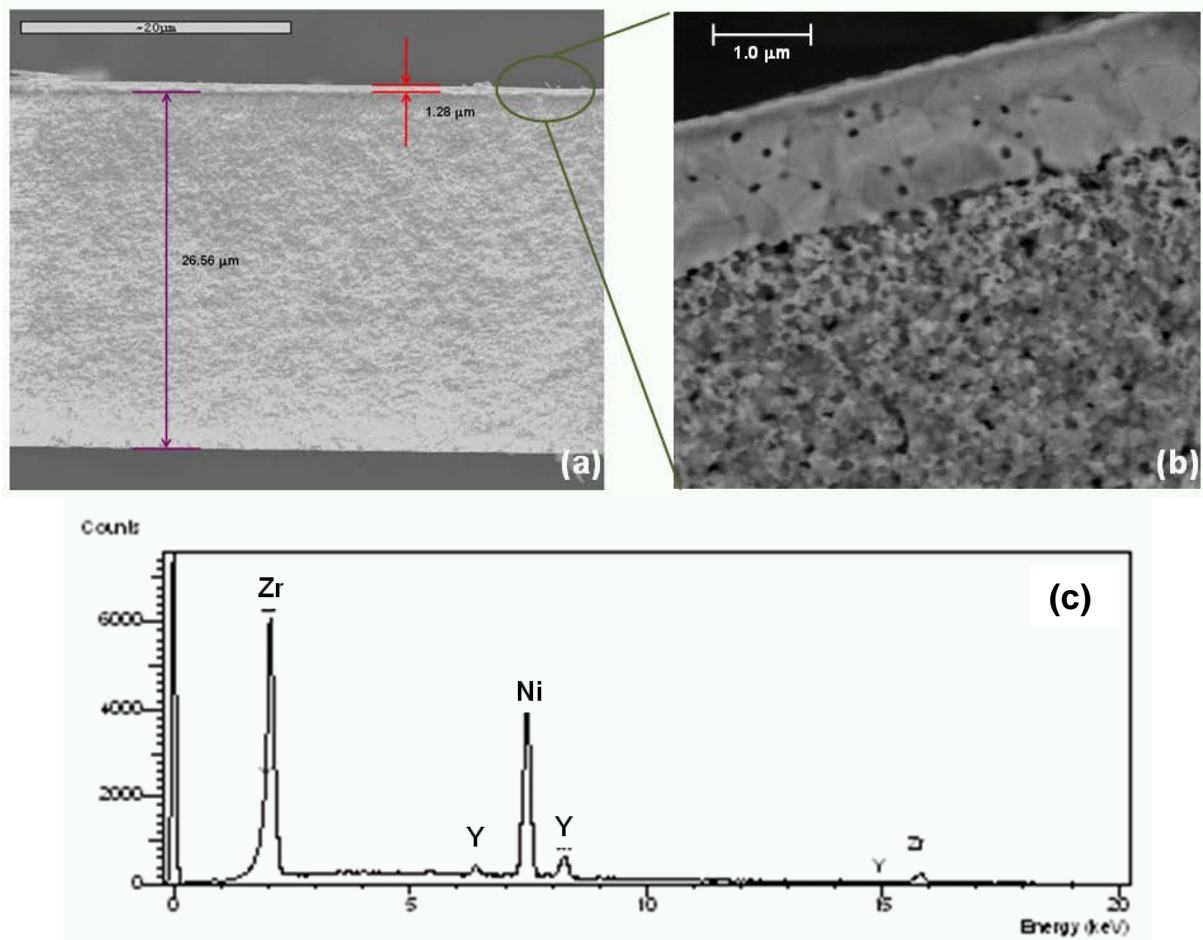


Figure 2. SEM photomicrographs: (a) secondary electrons image - 8YSZ/Ni-YSZ combined anode electrode-electrolyte ceramic sample; (b) backscattered electrons image - amplified region showing the 8YSZ/Ni-YSZ interface and the anode reaction zone. (c) X-ray dispersive energy spectroscopy (EDS) spectrum characteristic of ceramic combined system shown in Figure 2(a).

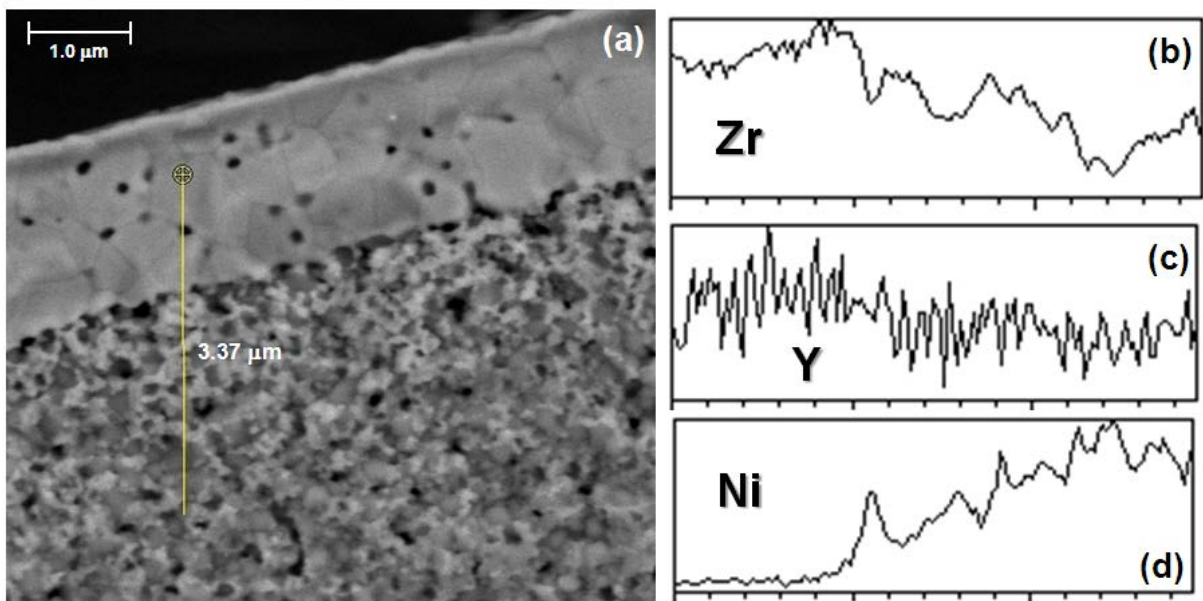


Figure 3. SEM-EDS Analysis: (a) backscattered electrons image - amplified region (Figure 2(b)) showing the 8YSZ/Ni-YSZ interface and the anode reaction zone, as well as the yellow line where EDS analysis was carried out; EDS spectrum for (b) Zr, (c) Y, and (d) Ni.

The microstructure of the anode can also be best seen in the photomicrographs shown in Figure 4, which show the porous nature of the structure, which is essential to ensure the percolation and diffusion of gas and the establishment of the triple-phase region (TPR),⁽⁶⁾ still providing thermal stability to the device.⁽¹⁷⁾

In fact, the characteristics of the transition region between the porous anode and dense electrolyte that ultimately characterize the interface 8YSZ/Ni-YSZ, are critical to ensure performance and stability for a SOFC.^(12,17) It should ensure that there is electrical connection available for ionic transport in this interface, without the existence of discontinuities that result in the establishment of impedances.^(6,18)

In this sense, the high densification of the electrolyte is essential^(12,19,20) Particularly in the photomicrographs of Figure 5 to identify clear grain boundaries, although in Figure 5(a) it is possible to identify any inter-and intragranular porosity, as seen in Figures 2(b) and 3(a). Since Figure 5(b) shows the absence of porosity and average grain size slightly less than the characteristic of Figure 5(a). The EDS spectrum shown in Figure 5(c) is associated with the photomicrograph of Figure 5(b) and indicates, as expected, only the elemental composition of the electrolyte, without contamination by Ni.

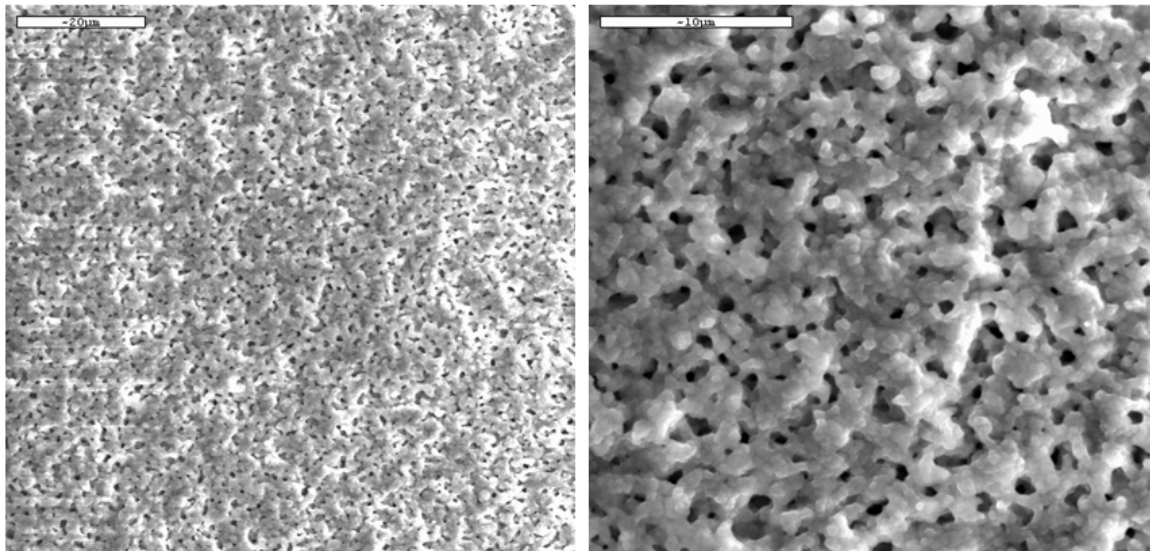


Figure 4. SEM photomicrographs (secondary electrons image) of the anodic electrode of the 8YSZ/Ni-YSZ combined electrodes-electrolyte ceramic.

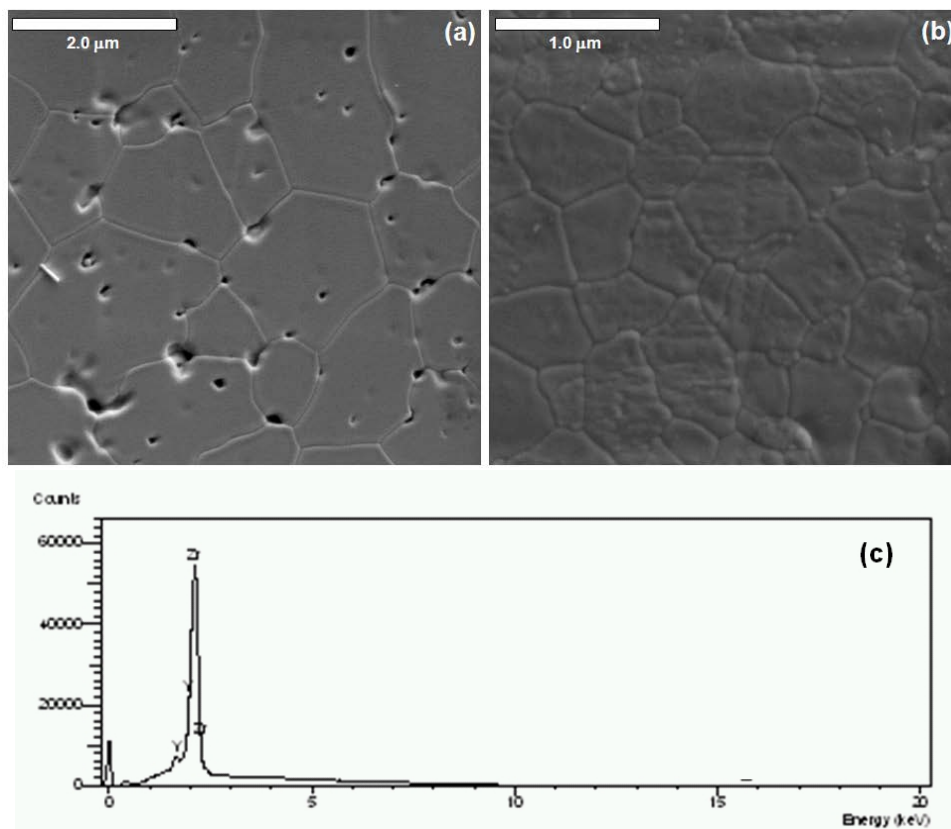


Figure 5. SEM micrographs of 8YSZ specimens sintered in different conditions: (a) showing mainly intergranular porosity; (b) showing a fully densified microstructure; (c) overall characteristic EDS spectrum.

Besides the traditional 8YSZ electrolyte, we have been also worked with electrolyte in the production of alternative combined electrode-electrolyte for application in intermediate temperature SOFC (IT-SOFC). Figure 6 shows a photomicrograph of the microstructure of a combined ERC/NiO produced by infiltration method and its chemical analysis by EDS of the electrolyte layer. The microstructure shows a distribution of porosity increasing from top to bottom, once the top layer is the electrolyte.

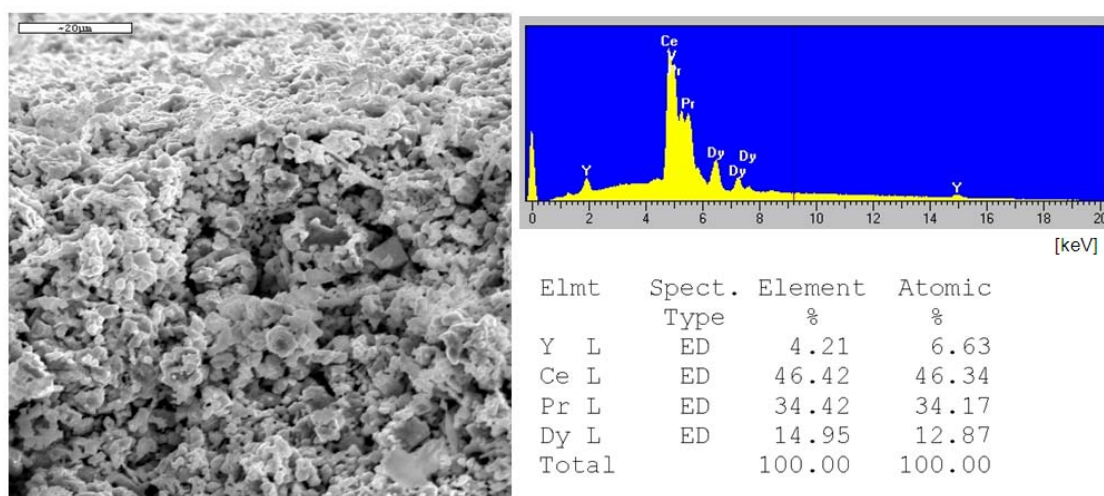


Figure 6. SEM micrographs of ERC/NiO combined bilayer produced by infiltration method and ceria-based electrolyte layer characteristic EDS spectrum.

Figure 7 shows the results of electrical characterization, showing the electrical resistances (ionic and electronic contact), in terms of their respective area-specific resistances (ASR), with respect to temperature (650-850^oC) and to chemical nature and thickness of the electrolyte. Figures 7(a) and 7(b) show, respectively, the ASR results when 8YSZ (a) and ERC (b) were employed as electrolytes. In both cases, the results for the lowest values of thickness (5 and 15 μm) of the electrolyte are also shown in detail separately (upper right part of the respective figures) for better observation. Figure 7(c) is complementary in nature and shows the ASR associated with the electrolyte/electrode interface and to total resistance of the single cell, showing both the average values and the total dispersion ranges.

The interfacial resistance includes the contact resistance between the electrode and the electrolyte as well as the resistance to the electrochemical processes such as charge transfer and mass transfer that taking place in the interface region⁽²¹⁾.

From the results of Figure 7, it is noted that, regardless of the physicochemical nature of the electrolyte (8YSZ or ERC), the shape of the dependence of resistance of the electrolyte in relation to the thickness thereof is very similar for both cases, although, especially in the interval 650-750^oC, the values of ASR for the ERC to be about of the half of those corresponding to 8YSZ, which corroborates the fact that ceria-based systems are suitable for IT-SOFC.^(15,19,22) Also, as the temperature increases the values of ASR are closer, especially for thicker electrolytes and values of the order of 0.02-0.05 $\Omega\cdot\text{cm}^2$ were obtained in the range of 700-850^oC for electrolytes with thickness of 5 μm .

Considering also the Figure 7(c) it can be seen that the ASR-related parameter is dominated by interface electrical resistance along the entire temperature range investigated, for thicknesses of 5 to 80 μm , resulting in greater contribution to the total ASR. Only for the largest thicknesses studied – 80 μm , only for 8YSZ, and 150 μm , for both electrolytes, – is that the contribution of the electrolyte was more significant. Thus demonstrating the negative impact of electrolytes thick to the power losses of SOFC systems, even more that the own total ASR values are higher for these conditions. The considerable dispersion of total ASR values is also indicative of a possible microstructural heterogeneity of the cells produced and processing studies further may possibly minimize these resistances.

Indeed, the power losses of the device are related to the electrothermal effects of microstructural origin, and from the results shown in Figure 8, it was noted that the power dissipated is almost directly proportional to the thickness of the electrolyte (size of the resistive path) and reversely proportional to the operating temperature of the system.

Additionally, for the systems evaluated, in virtually all conditions of temperature and thickness, the power dissipated was greater for the case of 8YSZ electrolyte. The differences between the values of dissipated power are greater, when the operating temperature is lower and practically these values tend to be equalized for the temperature of 850^oC. Particularly, at temperatures equals to 650 and 700, which have been considered for IT-SOFC systems, the results for cells with ERC as the electrolyte are better. Values of dissipated power density between 0.71 and 6.92 W/cm^2 were obtained, representing a variation of the results of the order of up to ten times, depending on operating temperature and the thickness of the electrolyte (Figure 8).

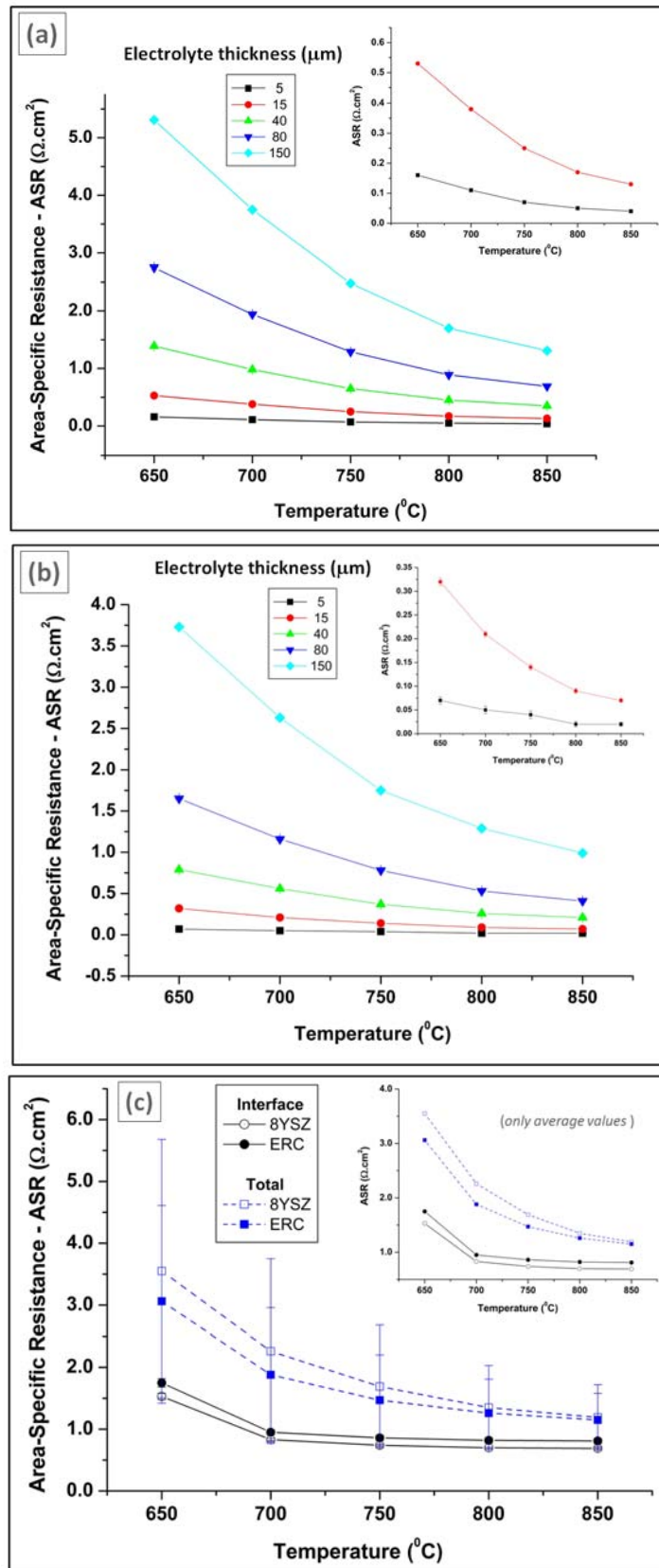


Figure 7. Electrical resistances – ionic or across of the electrolyte ((a) and (b), 5 and 15 μm of the thickness shown in the details), interfacial or material contact resistance and total resistance (c) with respect to temperature (650-850°C) and to nature and thickness of the electrolyte: (a) 8YSZ as electrolyte; (b) ERC as electrolyte; (c) interfacial and total resistances.

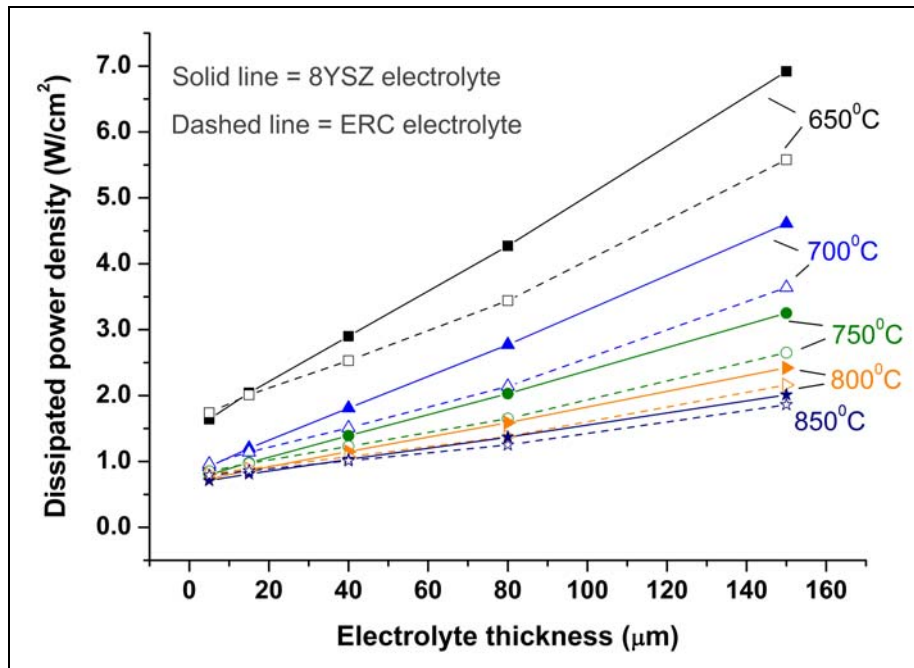


Figure 8. Dissipated power density of the single cells with respect to temperature (650-850°C) and to nature and thickness of the electrolyte - measurements made in an electric current density equal to 1 A/cm².

These analysis of area-specific resistance and dissipated power are complemented by the evaluation of the open-circuit voltage (OCV) provided by the single cell units, as shown in Figure 9, also as a function of temperature and thickness of the electrolyte.

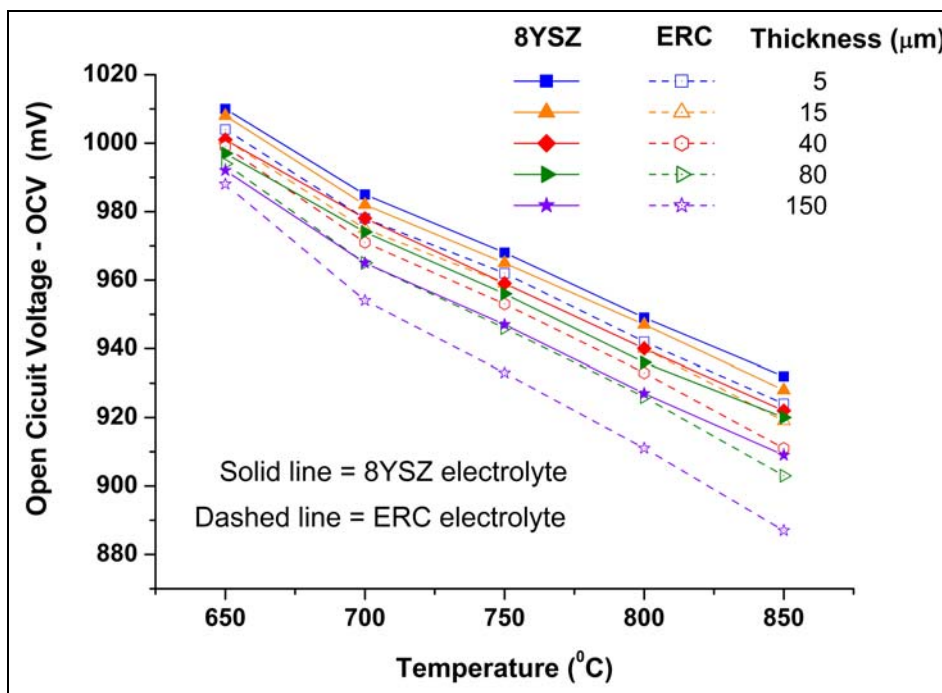


Figure 9. Open circuit voltage of the single cells with respect to temperature (650-850°C) and to nature and thickness of the electrolyte.

The results in Figure 9 show that the relation of the OCV with temperature is essentially linear, and in all cases studied, also the thinner electrolyte resulted in higher values for the OCV. However, in general, the OCV values were slightly higher in the cases of use of 8YSZ as electrolyte and the OCV values for the thickness of 150 μm (mainly for ERC) were significantly lower than for the other cases.

4 CONCLUSIONS

This work presented results of microstructural, compositional and electrothermal characterization of combined electrodes-electrolyte ceramics for application in solid oxide fuel cells with emphasis in the analysis of the influence of the thickness of the electrolyte on the electrical and electrochemical characteristics of the device. Microstructural analysis and evaluations of area-specific resistance, dissipated power and the open circuit voltage were performed. The results showed that it was possible to achieve significant reduction in electrical resistances when the thickness of the electrolyte is also significantly reduced. The best results were obtained with electrolyte of thickness equal to 5 mm for both to yttria-(8mol%)-stabilized zirconia (8 YSZ) and as to rare-earth-doped ceria (ERC). However, further studies about the degradation and aging of these materials still need to be made, as well as an evaluation on the dynamic behavior of fuel cells so produced.

REFERENCES

- 1 FAGHRI, A. Unresolved Issues in Fuel Cell Modeling. *Heat Transfer Engineering*, v.27, p. 1-3, 2006.
- 2 HOFFERT, M. I. Energy implications of future stabilization of atmospheric CO₂ content. *Nature*, v.395, p. 881-884, 1998.
- 3 CRABTREE, G. W., DRESSELHAUS, M. S., BUCHANAN, M. V. The Hydrogen Economy. *Physics Today*, Dec, 2004.
- 4 NEEF, H.-J. International overview of hydrogen and fuel cell research. *Energy*, V. 34, p. 327-333, March 2009.
- 5 ZINK, F., LU, Y., SCHAEFER, L. A solid oxide fuel cell system for buildings. *Energy Conversion and Management*, V. 48, p. 809-818, March 2007.
- 6 MINH, N. Q. Solid Oxide Fuel Cell Technology-Features and Applications, *Solid State Ionics*, v. 174. p. 271-277, 2004.
- 7 WINCEWICZ, K. C., COOPER, J. S. Taxonomies of SOFC material and manufacturing alternatives. *Journal of Power Sources*, 140, p.280-296, 2005.
- 8 SINGHAL, S. C., KENDALL, K. High temperature Solid Oxide Fuel Cells: Fundamentals, Design and Applications, Oxford, UK: Elsevier Ltd., p. 405, 2003.
- 9 IVERS-TIFFÉE, E., WEBER, A., SCHMID, K., KREBS, V. Macroscale modeling of cathode formation in SOFC. *Solid State Ionics*, v.174, n.1-4, p. 223-232, 2004.
- 10 STEELE, B. C. H., HEINZEL, A. Materials for fuel-cell technologies. *Nature*, v.414, p. 345-352, 2001.
- 11 HUSSAIN, M. M., LI, X., DINCER, I. A general electrolyte–electrode-assembly model for the performance characteristics of planar anode-supported solid oxide fuel cells. *Journal of Power Sources*, 189, p.916-928, 2009.
- 12 DESCLAUX, P., NÜRNBERGER, S., RZEPKA, M., STIMMING, U. Investigation of direct carbon conversion at the surface of a YSZ electrolyte in a SOFC. *International Journal of Hydrogen Energy*, 36, p. 10278–10281, 2011.
- 13 DING, J., LIU, J., YIN, G. Fabrication and characterization of low-temperature SOFC stack based on GDC electrolyte membrane. *Journal of Membrane Science*, 371, p. 219–225, 2011.

- 14 FUERTE, A., VALENZUELA, R. X., ESCUDERO, M. J., DAZA, L. Effect of cobalt incorporation in copper-ceria based anodes for hydrocarbon utilization in Intermediate Temperature Solid Oxide Fuel Cells. *Journal of Power Sources*, 196, p.4324-4331, 2011.
- 15 GIL, V., GURAUSKIS, J., CAMPANA, R., MERINO, R. I., LARREA, A., ORERA, V. M. Anode-supported microtubular cells fabricated with gadolinia-doped ceria nanopowders. *Journal of Power Sources*, 196, p.1184-1190, 2011.
- 16 NAKAJO, A., WUILLEMIN, Z., VAN HERLE, J., FAVRAT, D. Simulation of thermal stresses in anode-supported solid oxide fuel cell stacks - Part I: Probability of failure of the cells. *Journal of Power Sources*, 193, p. 203–215, 2009.
- 17 PIHLATIE, M., KAISER, A., MOGENSEN, M. Redox stability of SOFC: Thermal analysis of Ni–YSZ composites. *Solid State Ionics*, v.180, n.17-19, p.1100-1112, 2009.
- 18 LAURENCIN, J., DELETTE, G., SICARDY, O., ROSINI, S., LEFEBVRE-JOUD, F. Impact of 'redox' cycles on performances of solid oxide fuel cells: Case of the electrolyte supported cells. *Journal of Power Sources*, v.195, n.9, p.2747-2753, 2010.
- 19 PÉREZ-COLL, D., SÁNCHEZ-LÓPEZ, E., MATHER, G. C. Influence of porosity on the bulk and grain-boundary electrical properties of Gd-doped ceria. *Solid State Ionics*, v.181, n. 21-22, p. 1033-1042, 2010.
- 20 LIU, Y.L., HAGEN, A., BARFOD, R., CHEN, M., WANG, H. J., POULSEN, F. W., HENDRIKSEN, P.V. Microstructural studies on degradation of interface between LSM–YSZ cathode and YSZ electrolyte in SOFCs. *Solid State Ionics*, v.180, n. 23-25, p. 1298-1304, 2009.
- 21 XU, X., XIA, V., HUANG, S., PENG, D. YSZ thin films deposited by spin-coating for IT-SOFCs. *Ceramics International*, v.31, p. 1061-1064, 2005.
- 22 LARRAMENDI, I. R., ORTIZ-VITORIANO, N., ACEBEDO, B. Pr-doped ceria nanoparticles as intermediate temperature ionic conductors. *International Journal of Hydrogen Energy*, 36, p. 10981–10990, 2011.